SIAM J. Applied Dynamical Systems
Vol. 4, No. 4, pp. 1140–1158

The Motion of the Spherical Pendulum Subjected to a D_n Symmetric Perturbation*

Pascal Chossat† and Nawaf M. Bou-Rabee‡

Abstract. The motion of a spherical pendulum is characterized by the fact that all trajectories are relative periodic orbits with respect to its circle group of symmetry (invariance by rotations around the vertical axis). When the rotational symmetry is broken by some mechanical effect, more complicated, possibly chaotic behavior is expected. When, in particular, the symmetry reduces to the dihedral group D_n of symmetries of a regular n-gon, $n > 2$, the motion itself undergoes dramatic changes even when the amplitude of oscillations is small, which we intend to explain in this paper. Numerical simulations confirm the validity of the theory and show evidence of new interesting effects when the amplitude of the oscillations is larger (symmetric chaos).

Key words. spherical pendulum, elasticity, dihedral symmetry, reduction, nonlinear oscillations, chaos

AMS subject classifications. 34Cxx, 37Jxx, 70Kxx, 74Hxx

DOI. 10.1137/040616681

1. Introduction.

The spherical pendulum is a pendulum with a fixed length ℓ and an extremity consisting of a massive bob, which is allowed to move freely on the sphere of radius ℓ. In the subsequent analysis we are interested in the case when the angle of deviation of the pendulum with respect to its stable state of rest is small. We can therefore replace the spherical coordinates which define the position of the pendulum (the configuration space of this system is S^2) by the Cartesian coordinates on the horizontal (x, y) plane. We therefore set $z = -\sqrt{\ell^2 - x^2 - y^2}$ for the vertical coordinate (Figure 1).

This mechanical system with two degrees of freedom is a paradigm for integrable systems with symmetry [13]. It is very well-known that this system has two kinds of periodic motions: planar oscillations (in any vertical plane) and relative equilibria, which assume the form of circular motions in either one or the other direction of rotation around the vertical axis. These two kinds of periodic motion are "limiting" cases of quasi-periodic motions with two frequencies, where one frequency is related to the "oscillatory" behavior and the other one characterizes a "drift" around the vertical axis (precession). As is well known, when the ratio of these two frequencies is irrational, the motion is purely quasi-periodic (it never closes up), while if it is rational, the motion is in fact periodic (with, however, a period which can be very long). In experiments, it can be virtually impossible to distinguish between the truly quasi-periodic motions and the periodic ones. This behavior is a fundamental consequence of the

*Received by the editors October 10, 2004; accepted for publication (in revised form) by P. Holmes June 22, 2005; published electronically November 22, 2005.
http://www.siam.org/journals/siads/4-4/61668.html
†Institut Non Linéaire de Nice (CNRS UMR 6618), Sophia Antipolis, 06560 Valbonne, France, and Embassy of France in New Delhi, India (pascal.chossat@laposte.net).
‡Applied & Computational Mathematics, California Institute of Technology, Pasadena, CA 91125 (nawaf@acm.caltech.edu). This author was supported by a US DOE Computational Science Graduate Fellowship.

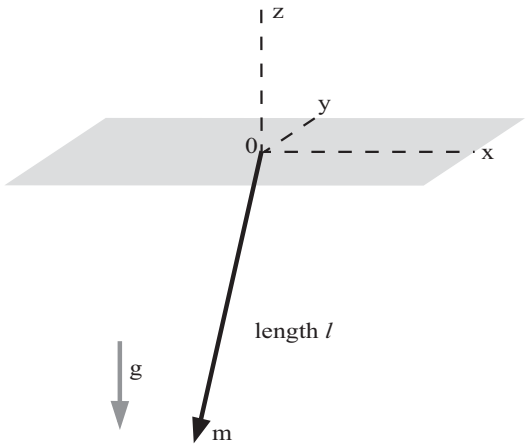

Figure 1. *The spherical pendulum.*

invariance of the energy (Hamiltonian function) through any rotation around the vertical axis (and reflection through any plane containing that axis). The symmetry group of the system is isomorphic to O(2), the group of 2×2 orthogonal matrices. The presence of rotational symmetry implies the existence of a first integral (conservation of angular momentum), which allows us to reduce the system to an integrable one. This will be recalled in section 3.

The following observation was made on a physical pendulum which can be found on the premises of the French embassy in New Delhi. It is part of a sculpture by Lalanne, and it consists of a long rod in bronze held (welded) in the hand of a centaur and terminated by a massive bob (Figure 2). The rod has hexagonal cross section. When this pendulum is moved away from its vertical position (state of rest), it oscillates in a vertical plane as expected, but after a while it starts rotating in one direction. Then after some other time, the rotational behavior decreases until the pendulum oscillates again in a vertical plane, different from the initial one. The whole sequence is then repeated, with the difference that now the pendulum rotates in the direction *opposite* to the previous one. This behavior repeats itself as long as there is enough energy to sustain a discernable motion. In term of coordinates in the (x, y) plane, the trajectories therefore follow the sequence which is schematized in Figure 3.

This behavior is clearly not compatible with the classical model of a spherical pendulum. What is the origin of this discrepancy? In Lalanne's pendulum, the rigid rod is clamped at its upper end (in the hand of the centaur); therefore the motion is due to elastic deformations. Nevertheless, if this system did satisfy the same O(2) invariance property as the spherical pendulum, we would expect that the dynamics would be similar and, in particular, that it would not exhibit alternating rotating oscillations. We mentioned that the rod had hexagonal cross section, which means that it has D_6 symmetry, where D_6 is the symmetry group of a regular hexagon. Our aim is to show how this fact can explain the unexpected motion of Lalanne's pendulum.

In the classical theory of rods it is assumed that (i) planar cross sections are transformed to planar cross sections (Bernoulli hypothesis) and (ii) Kirchhoff–Hooke linear constitutive equations hold. The former assumption allows for a drastic reduction of the number of kinematic

Figure 2. *The sculpture by Lalanne. The pendulum is held in the right hand of the centaur. Only small oscillations are permitted.*

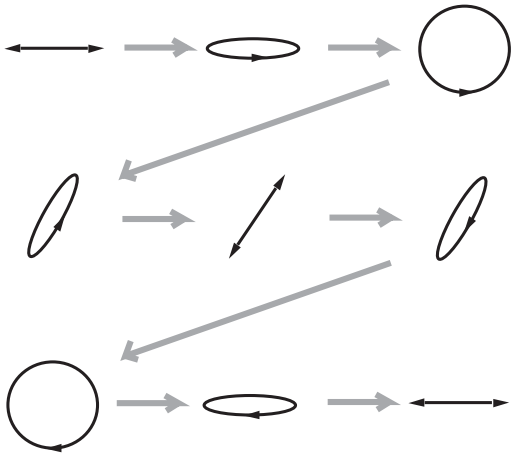

Figure 3. *The motion of the perturbed spherical pendulum projected on the horizontal plane.*

variables characterizing the deformations. In this case, however, since the principal moments of inertia of a regular n-gonal cross section ($n \geq 3$) are equal, the stored (elastic) energy function W has the same form as if the cross sections were $\mathrm{O}(2)$ invariant (see [3] for details). Such models are therefore not suitable for studying Lalanne's pendulum, and higher order effects should be taken into account. Moreover, it was shown in [6] that terms of order at least n in the Taylor expansion of W are required in order to distinguish between D_n and $\mathrm{O}(2)$ symmetry. The precise form of the D_n invariant terms will be recalled in section 4.

Following [3], where the compression of an inextensible and unshearable rod with D_n

symmetric cross section was studied, we may assume that a nonlinear, higher order moment/curvature (or stress/strain) relationship holds. Another possibility is to relax the hypothesis that planar cross sections are transformed to planar ones, thereby introducing a more complicated geometric description of the deformation (see also [7]). Whatever hypothesis is adopted to ensure D_n-symmetry of the model, we expect that it should lead to the same qualitative results.

In this paper we do not intend to derive and solve an exact model of Lalanne's pendulum. We shall instead exploit the fact that this system is close to being a spherical pendulum, thanks to the "large" aspect ratio of the rod (its length amounts to about 200 times its mean diameter) and to the presence of a massive bob at its lower end. We will then make the ansatz that the potential energy of the system can be written as the sum of the gravitational potential and of a D_6 (or more generally, D_n, $n \geq 3$) symmetric perturbation due to the elastic deformation, and we will show that such a system enjoys the same dynamics as the one observed with Lalanne's pendulum.

There are various ways in which an experiment can be mounted in order to precisely satisfy this hypothesis. For example, n identical springs can be attached to the rod at some distance ℓ_0 from its upper extremity and fixed to the "ceiling" at which the pendulum is suspended, and be equally distributed around the vertical axis. A similar idea was exposed in [7] for modeling elastic systems with discrete symmetry. Another possibility is to place the pendulum, the bob being a magnetic material (iron), into a magnetic field with D_n-symmetry (see [11] for a related study). In each of these experiments, the setup can be arranged so that its nonisotropic components act as a perturbation of the spherical pendulum. The potential energy V of the system can therefore be expressed as follows (under the above hypothesis on the amplitude of the oscillations):

$$V(x,y) = mg\left(\ell - \sqrt{\ell^2 - x^2 - y^2}\right) + \epsilon V_1(x,y), \tag{1}$$

where g is the acceleration of gravity, m is the mass of the bob, and V_1 is a D_n invariant smooth function. According to the above commentaries, this assumption implies that the Taylor expansion of V_1 contains terms of order at least n (see section 4 below). The number ϵ characterizes the "strength" of the perturbation potential. It depends on the mechanical system which is considered; for example, in the simulations of section 5 below, $\epsilon = k_e$ is proportional to the stiffness k of the springs. We can therefore write the Hamiltonian function of the system as

$$H_\epsilon(x,\dot{x},y,\dot{y}) = \frac{m}{2}\left(\dot{x}^2 + \dot{y}^2 + \frac{(x\dot{x}+y\dot{y})^2}{\ell^2 - x^2 - y^2}\right) + mg\left(\ell - \sqrt{\ell^2 - x^2 - y^2}\right) + \epsilon V_1(x,y). \tag{2}$$

Symmetry breaking of Hamiltonian systems of the kind we are considering here has been studied, for example, in [10], where the persistence of relative equilibria after a symmetry breaking perturbation has been applied to the system is investigated. Our point of view here is different: we wish to understand the effect of the perturbation on the motion of the system as it can be seen by an observer.

Our method to tackle the problem will be to find a suitable reduction of the dynamics for the spherical pendulum and for its perturbation. Basically, instead of reducing the dynamics

to the orbit space for the rotational group action in phase space, which does not persist after perturbation, we will restrict the analysis to the *normal form* of the Hamiltonian and project the system onto the quotient of the phase space by the S^1 action induced by the normal form transformation. This approximation will be justified if the following conditions are satisfied: (i) the energy is positive but small; (ii) the elapsed time of observation is not asymptotically long. These assumptions are compatible with the experimental observations. In the observation made on the sculpture in New Delhi's French embassy, only small departures from the vertical are possible. The fact that the perturbed system is nonintegrable and the dynamics may possess a chaotic behavior will not affect the main observation that this paper intends to understand.

We shall go through the following steps:

1. identify the suitable geometric framework for the normal form reduction of the problem;
2. describe the trajectories of the reduced system for the spherical pendulum;
3. analyze the effect of the reduced perturbation when setting $\epsilon > 0$;
4. reconstruct the motion from its reduced dynamics.

In order to explore the limit of validity of these assumptions, a set of numerical simulations has been carried out with an efficient variational integrator based on the work by Wendlandt and Marsden [14]. These simulations effectively reproduce the effect seen on Lalanne's pendulum when the amplitude of the oscillations is small enough. For larger amplitudes, chaotic effects manifest themselves and evidence for so-called symmetric chaos (as defined in [4]) is found. These numerical observations are described in the last section of the paper.

2. The geometric setup. We first identify the phase space with $\mathbb{C}^2$, and we put the Hamiltonian (2) into canonical form, by the following change of variables:

$$z_1 = \sqrt{\frac{mg}{2\ell}}(x + iy), \qquad z_2 = \sqrt{\frac{m}{2}}(\dot{x} + i\dot{y}).$$

Note that this corresponds to changing the time scale by a factor $\sqrt{\frac{\ell}{g}}$. When $\epsilon = 0$, the Hamiltonian is invariant under the action of the circle group O(2) defined by

$$\mathbf{R}_\varphi(z_1, z_2) = (e^{i\varphi} z_1, e^{i\varphi} z_2), \quad \varphi \in S^1, \tag{3}$$

$$\mathbf{S}(z_1, z_2) = (\bar{z}_1, \bar{z}_2), \tag{4}$$

which corresponds to the symmetries through the vertical axis of the pendulum. A third transformation

$$\mathbf{T}(z_1, z_2) = (z_1, -z_2) \tag{5}$$

leaves the Hamiltonian invariant and expresses the time reversibility of the system. When $\epsilon \neq 0$, the rotational invariance (3) is replaced by the n-fold symmetry

$$\mathbf{R}_{2\pi/n}(z_1, z_2) = (e^{2i\pi/n} z_1, e^{2i\pi/n} z_2). \tag{6}$$

Now the Hamiltonian function at $\epsilon = 0$ has the following quadratic leading part:

$$H_0(z_1, \bar{z}_1, z_2, \bar{z}_2) = z_1\bar{z}_1 + z_2\bar{z}_2 + 0(\|z_1\|^2 + \|z_2\|^2)^2. \tag{7}$$

We consider the normal form generated by this quadratic part. The corresponding linear vector field is

$$\begin{aligned} \dot{z}_1 &= -iz_2, \\ \dot{z}_2 &= iz_1, \end{aligned} \tag{8}$$

which generates the following action of the group S^1:

$$\tau(s)(z_1, z_2) = (z_1\cos(s) - z_2\sin(s), z_1\sin(s) + z_2\cos(s)). \tag{9}$$

Therefore, the normal form theory (which in this case is the same as averaging time over the period 2π) asserts that there exists a smooth near-identity change of variables which transforms the polynomial expansion of H_0, up to any order, into an S^1 invariant polynomial for the action of S^1 given by (9); see [2] for an exposition in the mechanical (Hamiltonian) context. From now on, H_0 will denote the (polynomial) normal form Hamiltonian function at $\epsilon = 0$, which therefore is invariant under the action of $\mathrm{O}(2) \times S^1$.

Now, we want to project the system onto the *orbit space* for the S^1 action in $\mathbb{C}^2$. For this we can use the following explicit formulation of the orbit space. We know that, S^1 being a compact group, the ring of S^1 invariant polynomials in $\mathbb{C}^2$, for the action defined in (9), is finitely generated. Some elementary algebra shows that a minimal family of generators is given by the four real terms π_j, $j = 1, \ldots, 4$, defined as follows:

$$\pi_c = \pi_1 + i\pi_2 = z_1^2 + z_2^2, \tag{10}$$

$$\pi_3 = z_1\bar{z}_1 + z_2\bar{z}_2, \tag{11}$$

$$\pi_4 = -i(z_1\bar{z}_2 - \bar{z}_1 z_2). \tag{12}$$

The map $\Pi : \mathbb{C}^2 \longrightarrow \mathbb{R}^4$ defined by $\Pi = (\pi_1, \pi_2, \pi_3, \pi_4)$ is called the Hilbert map of the S^1 action. It can be shown that its range is precisely diffeomorphic (as a stratified variety) to the orbit space. This method has been explained in the Hamiltonian context in [1]; see also [5] for a general exposition of the orbit space reduction method for equivariant dynamical systems. There must be one algebraic relation between these generators, which can easily be found:

$$\pi_1^2 + \pi_2^2 = \pi_3^2 - \pi_4^2. \tag{13}$$

Indeed, as a semialgebraic manifold, the dimension of the orbit space is equal to the dimension of the phase space, which is 4, minus the dimension of the typical S^1-orbits, which is 1. The above relation expresses this fact.

The S^1 invariance has an additional consequence, namely the existence of a first integral thanks to Noether's theorem; see [8], [13]. This quantity is the Hamiltonian function for the (Hamiltonian) vector field (8), i.e., the function π_3. Therefore by (13), the dynamics of the normal form are projected by the Hilbert map on the S^2 spheres $\pi_1^2 + \pi_2^2 + \pi_4^2 = I^2$, where I is any nonnegative number. This could be readily deduced from the fact that, in phase space, the condition $z_1\bar{z}_1 + z_2\bar{z}_2 = I$ defines an S^3 sphere and $S^3/S^1 \simeq S^2$. This sphere, at a given value of I, is what we call a *reduced orbit space*. We denote it by $\mathcal{S}_I$.

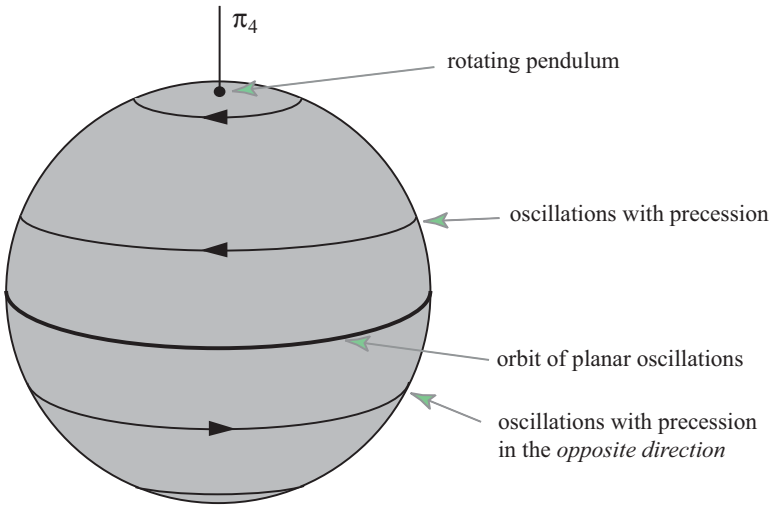

Figure 4. *The dynamics of the spherical pendulum in the reduced orbit space $\mathcal{S}_I$ and the corresponding motions.*

3. Motion of the unperturbed spherical pendulum. This case is well known (see, e.g., [13]); however, it is important to describe it first, in the geometric setting which we have introduced in the previous section, in order to further analyze the perturbed case.

Let us first look at the consequences of the spatial symmetries (3) and (4), which, as a matter of fact, hold for the full nonlinear problem (not just for the normal form). It is easily seen that these symmetries act on $\mathcal{S}_I$ as follows:

$$\mathbf{R}_\varphi(\pi_c, \pi_4) = (e^{2i\varphi}\pi_c, \pi_4), \tag{14}$$

$$\mathbf{S}(\pi_c, \pi_4) = (\bar{\pi}_c, -\pi_4). \tag{15}$$

We remark that the reflection S acts on $\mathcal{S}_I$ as a rotation by π. We will still call it a reflection in order to avoid any confusion.

Due to Noether's theorem, the vector field associated with the action of the rotations defined in (3) (or in (14)) possesses a first integral which is also a first integral for the unperturbed spherical pendulum. A simple calculation shows that this first integral is π_4 (conservation of the angular momentum). Therefore the planes $\pi_4 = const.$ are flow-invariant in the orbit space. It follows that, for a given value I, the trajectories in the orbit space are embedded in the intersections of these planes with the sphere $\pi_1^2 + \pi_2^2 + \pi_4^2 = I^2$ (see Figure 4). An equivalent way to arrive at this conclusion is by observing that, due to the $\mathrm{O}(2) \times S^1$ invariance, H_0 does not depend on π_c. Since H_0 (the energy of the unperturbed system) is a first integral, this implies that trajectories lie in the planes $\pi_4 = const.$

It remains to interpret this result and justify the commentaries written on Figure 4. We start with the equatorial circle. By (14) and (15), every point on this circle lies on the axis of a reflection which is conjugated to $\mathbf{S}$ by some rotation. It immediately follows that each of these points is an equilibrium in $\mathcal{S}_I$. It is therefore a relative equilibrium for the dynamics of the pendulum, and hence a periodic solution. The symmetry being conjugated to $\mathbf{S}$ is a reflection

in configuration space through the corresponding vertical plane. Therefore the corresponding motion in the (x, y) plane consists of oscillations along a segment of length $\sqrt{I/2}$, as can be easily checked. Note also that these relative equilibria are "orbitally stable." This means that if the initial condition of a solution is taken close enough to one of the equilibria lying on the equatorial circle, which is nothing but the orbit generated by the action of SO(2) on that equilibrium, then the corresponding forward trajectory will remain close, not to that particular equilibrium, but to the equatorial circle.

Now consider a circle above the equator. Points on this circle are no longer equilibria for the reduced dynamics. Since, however, the circle is an orbit under the action of $\mathbf{R}_\varphi$, $\varphi \in S^1$, we know that the solutions for the reduced dynamics must rotate at constant velocity along this circle. Lifting the dynamics back to phase space, the corresponding trajectories are relative periodic orbits lying on a 2-torus.

Let us now describe the motion in the horizontal plane. In a frame rotating with a suitable velocity around the π_4 axis, the trajectory for the reduced dynamics looks like a fixed point. Let us express this fact in the corresponding rotating frame in the horizontal plane. We may choose the rotating frame so that $\pi_1 = R \leq I$ and $\pi_2 = 0$ (therefore R is the radius of the circle in $\mathcal{S}_I$). By adding to these relations the condition that $\pi_3 = I$, we arrive at the following relation:

$$(I - R)x^2 + (I + R)y^2 = \frac{\ell}{mg}(I^2 - R^2), \tag{16}$$

which is the equation of an ellipse in the horizontal plane. In the limiting case $R = I$, which corresponds to being on the equatorial circle, the ellipse degenerates to a segment, which is what we had already found. In order to arrive at (16), it is convenient to set $z_j = r_j \exp i\psi_j$, $j = 1, 2$. From the condition $\pi_2 = 0$ we obtain

$$\cos^2(2\psi_2) = 1 - \frac{r_1^4}{r_2^4}\sin^2(2\psi_1),$$

and by $\pi_1 = R$ and $\pi_3 = I$ we get, using the above expression,

$$(I - r_1^2)^2 - r_1^4(1 - \cos^2 2\psi_1) = (R - r_1^2 \cos 2\psi_1)^2,$$

from which we finally get

$$2r_1^2(I - R\cos^2\psi_1 + R\sin^2\psi_1) = I^2 - R^2.$$

Since $z_1 = r_1(\cos\psi_1 + i\sin\psi_1) = \sqrt{\frac{mg}{2\ell}}(x + iy)$, the relation (16) follows.

In the fixed frame in the horizontal plane, the motion describes the well-known figure of an ellipsoidal curve which undergoes a constant drift after each "return" (the precession). When R tends to 0, i.e., when the circle on the sphere tends to the north pole (we assume here that $\pi_4 > 0$), the ellipse in the rotating frame tends to the circle of radius $\sqrt{I/2}$. In this limit, the solution is periodic (the pole is an equilibrium for the reduced dynamics), and the corresponding motion for the pendulum is a uniform rotation around the vertical axis. This solution is stable since the pole is a center.

Thanks to the reflection symmetry $\mathbf{S}$, which acts by (15) in the orbit space, the picture is similar in the southern hemisphere, with, however, an important difference: the direction of motion goes in the backward direction. Indeed, the southern hemisphere is also the image of the northern one by the time reversible symmetry $\mathbf{T}$, which transforms π_4 to $-\pi_4$ while keeping the other coordinates invariant. Therefore for a solution describing a circle between the equator and the south pole, the motion of the pendulum follows an ellipsoidal curve drifting in the direction *opposite* from that of the symmetric circle in the northern hemisphere.

4. Motion of the perturbed spherical pendulum. We now come back to the perturbed Hamiltonian, which we write $H_\epsilon = H_0 + \epsilon V_1$ (see (2)), where ϵ is a fixed positive coefficient that we may choose as small as we wish. The potential V_1 being invariant under the action of D_n in the (x, y) plane, its leading part is quadratic: using the complex z_1 variable, we can write $V_1(z_1, \bar{z}_1) = az_1\bar{z}_1 + 0(\|z_1\|^4)$. Therefore the leading part of the function H_ϵ is $(1+\epsilon a)z_1\bar{z}_1 + z_2\bar{z}_2$. For ϵ small enough, the normal form theory for H_ϵ is the same as for H_0. In other words, the normal form is again an invariant function for the S^1 action given by (9), up to a rescaling of time. For the sake of simplicity, we keep the same notation for the normal form, which we can now express in terms of the invariants π_j, $j = 1, \ldots, 4$:

$$H_\epsilon(\pi_1, \pi_2, \pi_3, \pi_4) = H_0(\pi_3, \pi_4^2) + \epsilon\widetilde{H}(\pi_1, \pi_2, \pi_3, \pi_4^2), \tag{17}$$

where $\widetilde{H}$ is invariant under the action of D_n in the orbit space defined by the transformations

$$\mathbf{R}_{2\pi/n}(\pi_c, \pi_3, \pi_4) = (e^{4i\pi/n}\pi_c, \pi_3, \pi_4), \tag{18}$$

$$\mathbf{S}(\pi_c, \pi_3, \pi_4) = (\bar{\pi}_c, \pi_3, -\pi_4), \tag{19}$$

and we recall that $\pi_c = \pi_1 + i\pi_2$. Note that when n is odd, these relations define on the plane $(\pi_c, \bar{\pi}_c)$ an irreducible representation of D_n, while for n even, they define an irreducible representation of $D_{n/2}$. From now on we set $k = n$ if n is odd and $k = n/2$ if n is even. It is a classical exercise to show that, thanks to the D_k invariance, $\widetilde{H}$ can be expressed as a polynomial in $\pi_c\bar{\pi}_c$, $\mathrm{Re}(\pi_c^k)$, π_3, and π_4^2 (see [5] and [9]).

The invariant function π_3 is still a first integral of the motion, thanks to the S^1 invariance of the Hamiltonian normal form (Noether's theorem), and we can still study the dynamics in the reduced orbit space $\mathcal{S}_I$ defined by (13). Let us first notice that there are now $k+1$ axes of symmetry in the space spanned by (π_1, π_2, π_4) in which $\mathcal{S}_I$ is embedded. One of them is the vertical axis passing through the poles, which implies that these poles are still relative equilibria for the perturbed system. Moreover, these equilibria are still stable (centers) because the perturbation is small. The other axes of symmetry lie in the horizontal (equatorial) plane and are remnants of the continuum of axes of symmetry which filled this plane when $\epsilon = 0$. Therefore there are $2k$ (relative) equilibria uniformly distributed on the equator. Thanks to the Poincaré–Hopf index theorem (and because the Euler characteristic of the 2-sphere is 2) and by an argument of symmetry, we can claim that, except if additional degeneracies are present in the problem (a case which we can discard here), these equilibria must alternate saddles and centers.

It should be remarked that the relative equilibria which we have found correspond to periodic orbits which persist when the remainder is added to the normal form in the Hamiltonian

system. The proof of persistence proceeds as a generalization of the Moser–Weinstein theorem and can be found in [12]. These periodic solutions can be classified according to their isotropy types (their conjugacy classes of isotropy subgroups), as laid out in [9] for Hopf bifurcation with D_n symmetry. In the classical approach, periodic solutions are sought in invariant subspaces, which are defined as the sets of points (in phase space) which are fixed under the action of isotropy subgroups of $D_n \times S^1$ (symmetry of the normal form). Here we first project the normal form onto the (reduced) orbit space $\mathcal{S}_\mathcal{I}$ for the S^1 action. The isotropies and the form of these solutions can also be reconstructed from the corresponding singularities on the orbit space. Each point on $\mathcal{S}_\mathcal{I}$ corresponds to an S^1 orbit in phase space, according to the action of S^1 defined by (9). As shown in [9], the isotropy subgroup of such a periodic solution is either purely spatial, i.e., a subgroup of D_n, or is a "spatiotemporal" subgroup of $D_n \times S^1$ generated by an element of the form $(\gamma, 2\pi/m)$, where γ is an element of order $m > 1$ in D_n. In fact, when n is even, any point in phase space is fixed by the element $(\mathbf{R}_\pi, \pi)$, which can therefore be forgotten in the classification by isotropy types in this case.

We leave it to the reader to check that the two equilibria at the poles are the images, under the Hilbert map Π, of n-folded discrete "rotating waves." Such solutions are characterized by their spatiotemporal symmetry $(\mathbf{R}_{2\pi/n}, -2\pi/n)$: if $X(t)$ denotes the solution, then $\mathbf{R}_{2\pi/n} X(t - 2\pi/n) = X(t)$ for all t. The corresponding motion in the (x, y) plane looks like a deformed circle with n-fold symmetry.

Let us now consider the (relative) equilibria lying on the equatorial circle of $\mathcal{S}_\mathcal{I}$. In the unperturbed case, every point on the equator is a (relative) equilibrium, and we have seen in the previous section that every corresponding pendulum's motion is a planar oscillation. This comes from the condition $\pi_4 = 0$ and it is still true for the surviving (relative) equilibria on the equator in the perturbed case. Each of these equilibria is characterized by the fact that it belongs to an axis of reflection symmetry for the group D_k acting like (18)–(19) in the space spanned by (π_1, π_2, π_4). For a given axis of symmetry, there are two such equilibria which are diametrically opposite.

When k is even, every pair of such diametrically opposite equilibria is formed from images of each other by the rotation by π in D_k. Therefore the corresponding periodic solutions must have the same isotropy type in phase space. There are, however, two different types of reflection symmetry in D_k: the type $\mathbf{S}$ (as defined in (19)) and the type $\mathbf{R}_{2\pi/k}\mathbf{S}$. We leave it to the reader to check that in the first case, the isotropy type of the periodic solution is $\mathbf{S}$ (meaning the group generated by this order 2 element acting in phase space), while in the second case, the isotropy type is $\mathbf{R}_{\pi/k}\mathbf{S}$. Therefore the planes of oscillations of the pendulum are the planes of reflection symmetry for the action of D_n in configuration space.

When k is odd, there is only one isotropy type for the singularities on the equator in $\mathcal{S}_\mathcal{I}$, and this type is defined by the reflection $\mathbf{S}$. However, the diametrically opposite equilibria, which belong to the same reflection axis, are not symmetric to each other in this case. When lifting these points back to phase space, it can be checked that one of them corresponds to solutions with isotropy type $\mathbf{S}$, while the other one corresponds to the spatiotemporal isotropy type $(\mathbf{S}, \pi)$. As shown in [9], in the case when n is also even (i.e., when $n = 2 \bmod (4)$), the element $(\mathbf{S}, \pi)$ is in fact conjugated to $\mathbf{R}_{\pi/k}\mathbf{S}$.

The task is now to study what the phase portrait looks like away from these equilibria.

An invocation of the Poincaré–Bendixson theorem would be sufficient to fully describe the

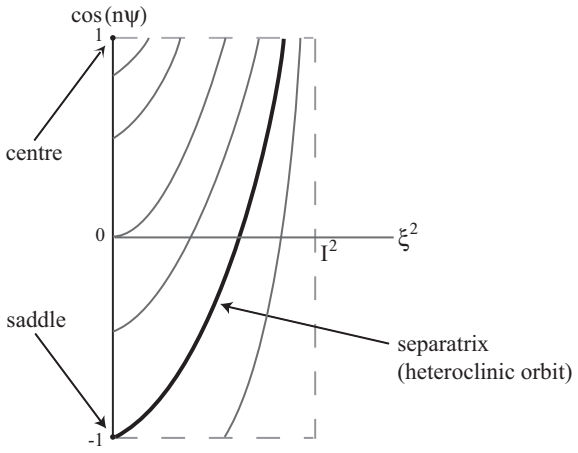

Figure 5. *The curves defined by* (21) *when* E *is varied.*

phase portrait. We may also be more explicit and notice that there are still two first integrals in the problem: $\pi_3 = I$ and conservation of the energy, $H_\epsilon = E$. Let us express the Taylor expansion of the second relation, with π_3 replaced by I and taking account of the fact that, as mentioned earlier, $\widetilde{H}$ and therefore H_ϵ is a function of $\pi_c\bar{\pi}_c$, $\mathrm{Re}(\pi_c^k)$, and π_4:

$$E = I + \alpha\pi_4^2 + 0(\pi_4^4) + \epsilon\beta\mathrm{Re}(\pi_c^k)[1 + 0(|\pi_c|^2 + \pi_4^2)]. \tag{20}$$

We shall assume that the coefficients α and β, which depend upon the system under consideration, are nonvanishing. By setting $\pi_c\bar{\pi}_c = I^2 - \pi_4^2$ (see the relation (13)), $\pi_c = \rho\exp(\psi)$, and $\pi_4 = \xi$ (for the sake of notational clarity), we are led to solve an equation of the form

$$E = I + \alpha\xi^2 + \epsilon\beta(I^2 - \xi^2)^{k/2}\cos(k\psi). \tag{21}$$

The higher order terms can be neglected as long as the first integrals E and I are assumed to be small. The only quantity which can still be varied is the energy E. This defines a family of curves that typically look like those in Figure 5. Each curve represents a trajectory in $\mathcal{S}_I$. The identification of the various equilibria in this picture is easy. The points at $\xi = 0$ and $\cos k\psi = \pm 1$ represent the two types of equilibria on the equatorial circle. The curve which starts from the lower point ($\xi = 0$ and $\cos k\psi = -1$) is a separatrix for the dynamics. By symmetry, it corresponds in $\mathcal{S}_I$ to a trajectory connecting two saddles, and therefore to a heteroclinic orbit. The curves lying above the separatrix correspond to periodic orbits winding around the (relative) equilibrium sitting at the pole. In the asymptotic limit $\xi = I$, the curves tend to this equilibrium. The curves which lie below the separatrix correspond to periodic orbits winding around the centers on the equator. By reflection symmetry, the phase portrait is the same in both hemispheres, with only a time reversal. The phase portrait in $\mathcal{S}_I$ is sketched in Figure 6.

It can be concluded that the dynamics are not much affected by the perturbation $\epsilon \neq 0$ near the rotating solution of the spherical pendulum, while they are completely modified near its planar oscillations.

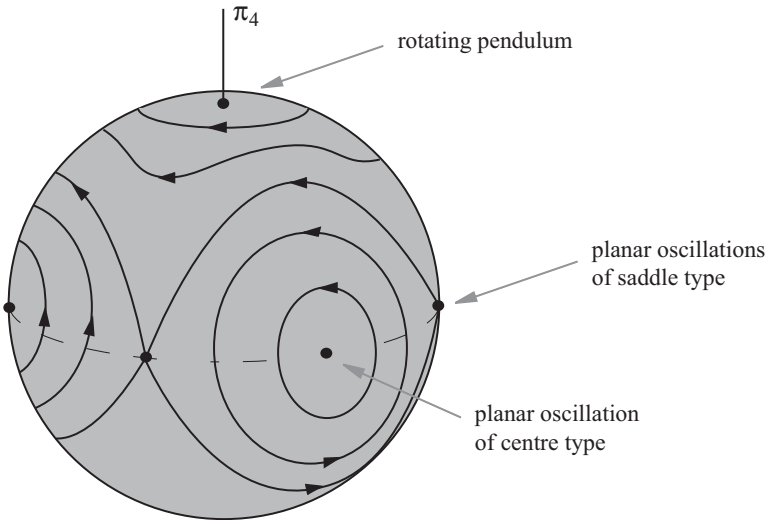

Figure 6. *The phase portrait in the reduced orbit space $\mathcal{S}_I$.*

It remains to reconstruct the motion of the pendulum from these reduced dynamics, when the initial condition is taken as in the experimental observation.

Let us therefore consider the case when the pendulum is just moved away from its vertical position, with no initial velocity. This corresponds to taking an initial condition on the equatorial circle for the reduced dynamics. Here it is useful to remark that π_4 is, up to a scalar factor, the vector product of the position (x, y) in the horizontal plane by the velocity $(\dot{x}, \dot{y})$. Therefore the condition $\pi_4 = 0$ implies that the velocity is aligned with the position vector. It follows that the pendulum starts moving in the vertical plane carrying its initial position (or, in the (x, y) plane, along the line of intersection of these two planes). Except at the exceptional points corresponding to the equilibria themselves, the trajectory in $\mathcal{S}_I$ follows one of the closed orbits surrounding one of the centers positioned on the equator. Hence the forward trajectory moves away from the equator, entering, for example, the northern hemisphere. This means, as follows from the discussion of the unperturbed case, that a rotating component will be superposed to the planar oscillation, inducing a drift with a positive angle, say. As long as the solution is very close to the equator, the ellipsoid looks very much like a segment (planar oscillations), but as the solution moves away from the equator, the motion in the horizontal plane comes closer to a circle. After a while the solution again approaches the equator, meaning that the ellipsoid flattens until it again looks like a segment. After crossing the equator to enter the southern hemisphere, the same evolution of the motion will be observed, but in the *reverse* direction, due to the time reversing symmetry T, which corresponds to reflection symmetry through the equator in the reduced orbit space. If, in the horizontal plane, the initial condition makes an angle θ with the direction of the stable planar oscillations which are next to this initial condition, then, just before the drift changes direction, the motion is aligned along a segment that makes an angle $-\theta$ with these planar oscillations. The solution is quasi-periodic with two frequencies. Of course the frequencies may be rationally related, in which case the quasi periodicity degenerates into periodicity. The evolution in the horizontal

plane looks like that in Figure 3. In the case of Lalanne's sculpture, quasi periodicity versus periodicity or irregular motion is very difficult to assert due to the relatively short life time and small amplitude of the oscillations.

5. A numerical exploration of the D_n-perturbed spherical pendulum. The model we investigate in this section is the spherical pendulum (bob of mass m, length ℓ) attached to an inertial frame of reference at O, with n springs (spring constants k) symmetrically attached to the pendulum at a distance ℓ_0 from O. We set $\ell_0 = \alpha\ell$ with $\alpha < 1$. Figure 7 shows the case where $n = 2$.

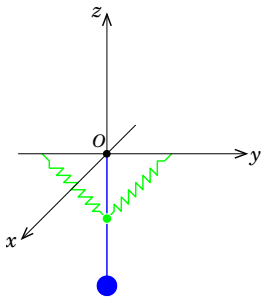

Figure 7. *Sketch of a pendulum with D_2 symmetry.*

Here we do not restrict the computations to the normal form nor to very small amplitude oscillations. The aim of this section is to explore the domain of validity of the theory which has been laid out in the previous sections, as well as the behavior of the system beyond this domain of validity.

The configuration space of this system is S^2, and its Lagrangian is given by

$$L(\mathbf{x}, \dot{\mathbf{x}}) = \frac{1}{2}\dot{\mathbf{x}}^T\dot{\mathbf{x}} - \mathbf{x}^T\mathbf{e}_z - \frac{k_e}{2}\sum_{i=1}^{n}(\sqrt{2} - \|\mathbf{x} - \mathbf{p}_i\|)^2,$$

where time has been rescaled by the gravitational time scale $\sqrt{\ell/g}$ and position by the length scale ℓ; $k_e = k\alpha^2\ell/mg$; and $\mathbf{p}_i$ is the unit position vector of the endpoint of the ith spring at $z = 0$, where $i = 1, \ldots, n$.

In particular, for $n = 4$ the D_4 symmetric potential is given explicitly by

$$V(\mathbf{x}) = k_e\left(8 - 2\sqrt{1 - \mathbf{x}^T\mathbf{e}_x} - 2\sqrt{1 + \mathbf{x}^T\mathbf{e}_x} - 2\sqrt{1 - \mathbf{x}^T\mathbf{e}_y} - 2\sqrt{1 + \mathbf{x}^T\mathbf{e}_y}\right).$$

This potential is invariant under the discrete symmetry given by

$$V\left(\mathbf{R}_z\left(\frac{n\pi}{2}\right)\mathbf{x}\right) = V(\mathbf{x})$$

for $n \in \mathbb{Z}^+$ and where $\mathbf{R}_z(\theta)$ is the rotation about the vertical by the amount θ.

For $n = 6$ the D_6 symmetric potential is given explicitly by

$$V(\mathbf{x}) = k_e \Big(12 - 2\sqrt{1-\mathbf{x}^T\mathbf{e}_x} - 2\sqrt{1+\mathbf{x}^T\mathbf{e}_x} \\ - \sqrt{2}\sqrt{2-\mathbf{x}^T\mathbf{e}_x - \sqrt{3}\mathbf{x}^T\mathbf{e}_y} - \sqrt{2}\sqrt{2+\mathbf{x}^T\mathbf{e}_x - \sqrt{3}\mathbf{x}^T\mathbf{e}_y} \\ - \sqrt{2}\sqrt{2+\mathbf{x}^T\mathbf{e}_x + \sqrt{3}\mathbf{x}^T\mathbf{e}_y} - \sqrt{2}\sqrt{2-\mathbf{x}^T\mathbf{e}_x - \sqrt{3}\mathbf{x}^T\mathbf{e}_y} \Big).$$

This potential is invariant under the discrete symmetry given by

$$V\left(\mathbf{R}_z\left(\frac{n\pi}{3}\right)\mathbf{x}\right) = V(\mathbf{x})$$

for $n \in \mathbb{Z}^+$ and where $\mathbf{R}_z(\theta)$ is a rotation about the vertical by the amount θ.

To variationally integrate we define the *discrete Lagrangian*

$$\mathbb{L}(\mathbf{x}_{k+1}, \mathbf{x}_k) = L\left(\mathbf{x}_k, \frac{\mathbf{x}_{k+1}-\mathbf{x}_k}{h}\right) \\ = \frac{1}{h^2}(1 - \mathbf{x}_{k+1}^T\mathbf{x}_k) - \mathbf{x}_k^T\mathbf{e}_z - V(\mathbf{x}_k) \tag{22}$$

and *unconstrained action sum* $\mathbb{S} = \sum_{k=0}^{N-1} \mathbb{L}(\mathbf{x}_{k+1}, \mathbf{x}_k)$. The difference scheme is obtained by extremizing $\mathbb{S}$, subject to the constraint that $\mathbf{x}_k \in S^2$, i.e., $g(\mathbf{x}_k) = \mathbf{x}_k^T\mathbf{x}_k - 1 = 0$. The resulting update scheme is implicit and locally second order accurate. See Wendlandt and Marsden [14] for more theory.

For small values of the energy our simulations confirm the results of the previous sections and the relevance of the normal form reduction to analyzing the n-fold symmetric Hamiltonian dynamics. This is well illustrated in Figures 8(a)–8(c) in the square symmetry case ($n = 4$), and in Figures 9(a)–9(c) in the hexagonal symmetry case ($n = 6$). These figures show the trajectories projected onto the horizontal (x, y) plane for various initial conditions (with inital velocity set to 0). Observe that when the initial condition is taken close to the periodic orbit corresponding to a saddle equilibrium on the reduced orbit space (Figures 8(c) and 9(c)), then the alternating dynamics which have been investigated in the previous sections are clearly shown: the pendulum oscillates for a while along the unstable periodic orbit, then starts rotating with a precession driving it to another "nearby" unstable periodic orbit, and the process repeats itself in the opposite direction. (In Figure 8(c), for example, these periodic orbits correspond to the vertical and horizontal oscillations.)

The simulation movies of the motion corresponding to Figures 8(c) and 8(d) for $n = 4$ and Figures 9(c) and 9(d) for $n = 6$ can be downloaded from http://www.acm.caltech.edu/~nawaf.

Observe that when the initial condition is taken very close to an unstable periodic orbit, as in Figures 8(d) and 9(d), the same alternating dynamics are observed, but now the pendulum follows an erratic trajectory, exploring the vicinity of *all* unstable periodic oscillations and *all* regions delimited by these oscillations in the (x, y) plane. The trajectory seems to retrieve the initial D_n-symmetry of the system asymptotically. This is reminiscent of "symmetric chaotic dynamics," a phenomenon which has been thoroughly investigated after it was identified by [4] in 1988. This would indicate that even at small values of the energy, chaotic dynamics are created near these unstable periodic orbits.

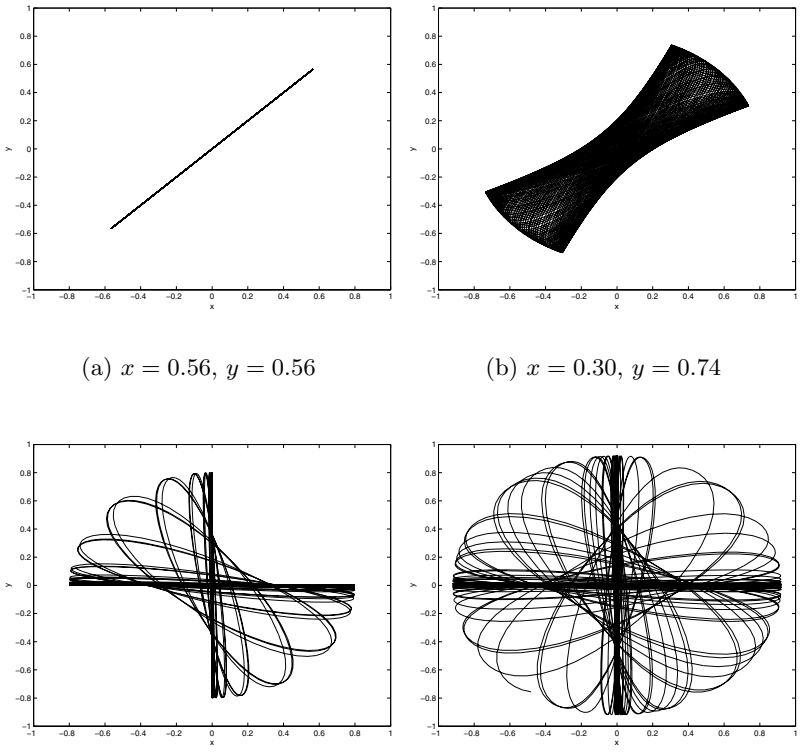

(a) $x = 0.56$, $y = 0.56$ (b) $x = 0.30$, $y = 0.74$

(c) $x = -8 \cdot 10^{-8}$, $y = 0.8$ (d) $x = -9.2 \cdot 10^{-8}$, $y = 0.92$

Figure 8. *Aerial views of the trajectory of the spherical pendulum bob for solutions initially at rest at the positions shown in the subcaptions under a potential with D_4 symmetry. Note: $t \in [0, 400]$, $\Delta t = 0.0062$, and $k_e = 0.4$.*

In order to confirm this conjecture, we have computed a Poincaré section for the dynamics around the unstable periodic orbit defined by setting $y = dy/dt = 0$ and for fixed total energy. Therefore the Poincaré section is in the plane $(y, dy/dt)$. We assume that the minimum value of the energy is that of the hanging pendulum ($H = -1$). The results are shown in Figures 10 and 11. For a value of H close to the minimum, the Poincaré section is mostly foliated by closed orbits corresponding to invariant tori (quasi-periodic oscillations) with the exception of irregular orbits which pass close to the central saddle. For larger values of H, this irregular region of the dynamics becomes more visible. The numerical evidence of transverse intersections of stable and unstable manifolds of the central saddle is shown in Figures 12 and 13, where several iterates of a small disk around the saddle at the origin (corresponding to the unstable periodic oscillation at which the Poincaré section is taken) are plotted. The trajectories show typical tangles due to transverse intersections of the stable and unstable manifolds of the saddle at the origin. The authors intend to investigate this question in more detail in a forthcoming work.

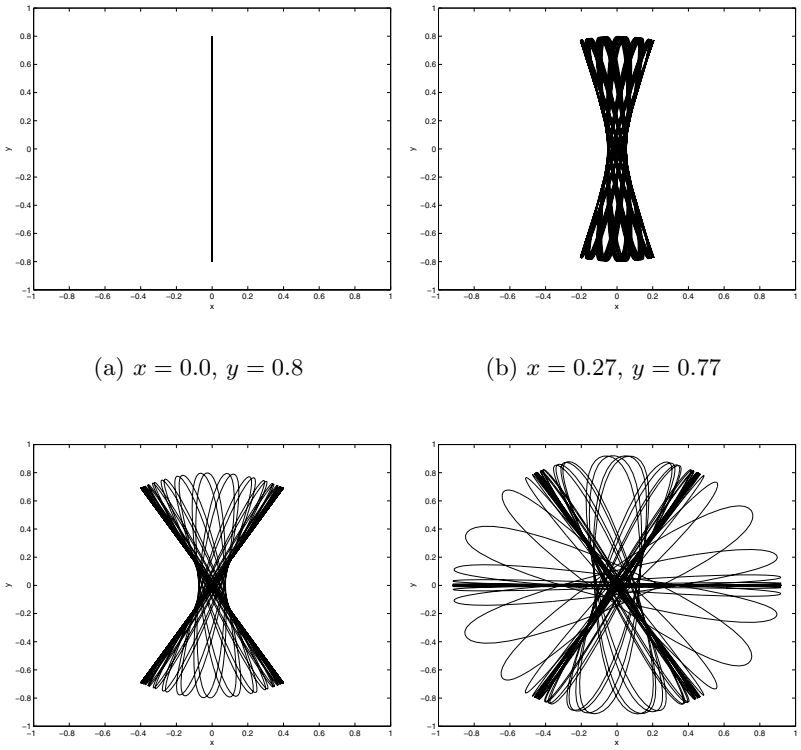

(a) $x = 0.0$, $y = 0.8$ (b) $x = 0.27$, $y = 0.77$

(c) $x = 0.39$, $y = 0.69$ (d) $x = 0.45$, $y = 0.79$

Figure 9. *Aerial views of the trajectory of the spherical pendulum bob for solutions initially at rest at the positions shown in the subcaptions under a potential with D_6 symmetry. Note: $t \in [0, 400]$, $\Delta t = 0.0062$, and $k_e = 0.4$.*

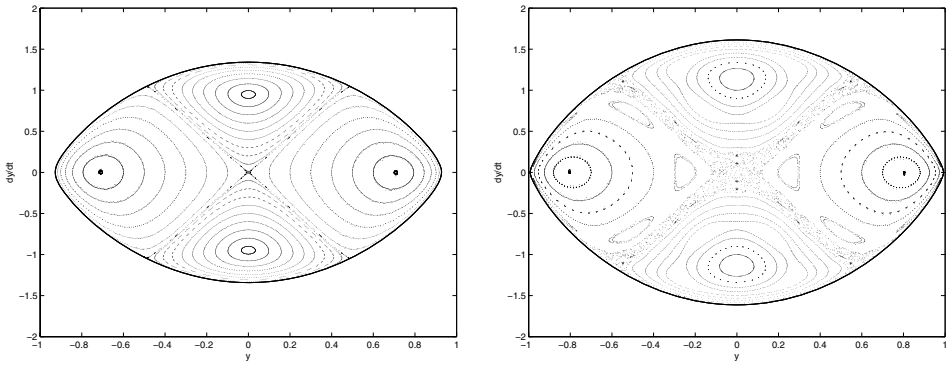

(a) $H = -0.1$ (b) $H = 0.3$

Figure 10. *Poincaré sections of a spherical pendulum under a potential with D_4 symmetry. Here $k_e = 0.4$.*

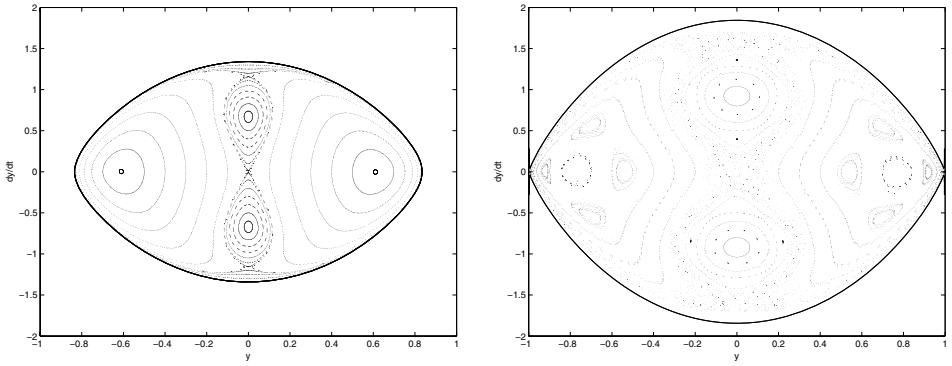

(a) $H = -0.1$ (b) $H = 0.7$

Figure 11. *Poincaré sections of a spherical pendulum under a potential with D_6 symmetry. Here $k_e = 0.7$.*

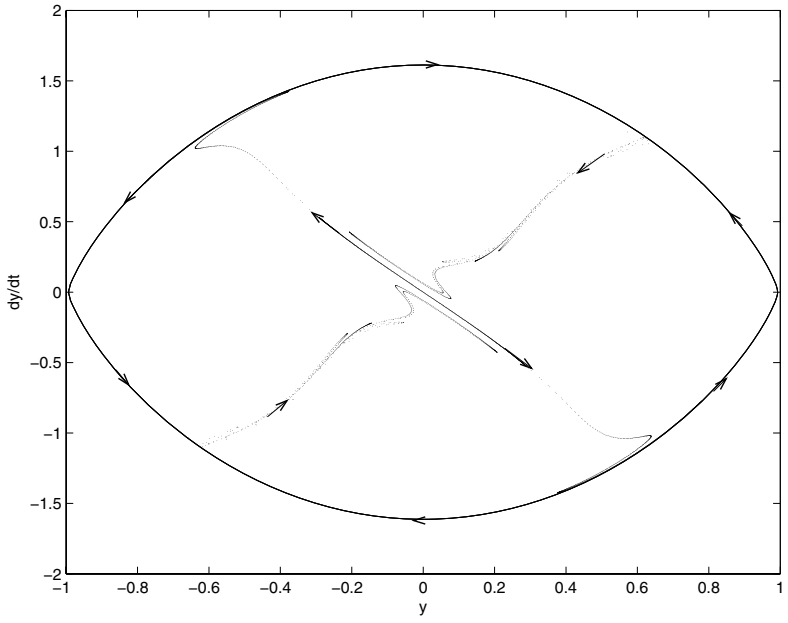

Figure 12. *The stable and unstable manifolds through the central saddle with arrows indicating the direction of the flow for the spherical pendulum under a potential with D_4 symmetry. Here $k_e = 0.4$, $H = 0.3$.*

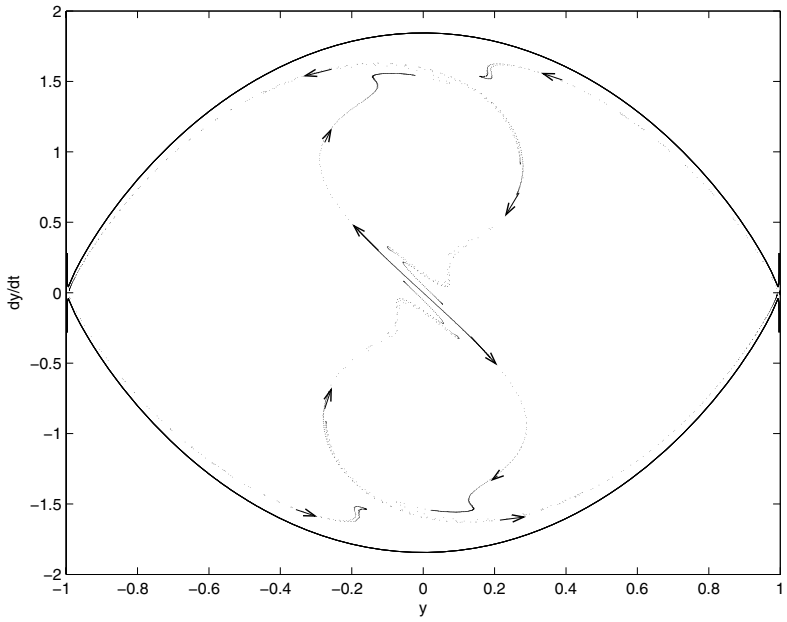

Figure 13. *The stable and unstable manifolds through the central saddle with arrows indicating the direction of the flow for the spherical pendulum under a potential with D_6 symmetry. Here $k_e = 0.7$, $H = 0.7$.*

Acknowledgments. The authors are grateful to Jerry Marsden for his interest in this work and for having suggested Nawaf Bou-Rabee to undertake the numerical part. P. Chossat is grateful to the Ambassador of France in India, Mr. Dominique Girard, for allowing him to take a picture of the centaur, and for his support. Both authors are grateful to Phil Holmes, Gabor Domokos, and Tim Healey for their insightful comments.

REFERENCES

[1] J. M. Arms, R. Cushman, and M. J. Gotay, *A universal reduction procedure for Hamiltonian group actions*, in The Geometry of Hamiltonian Systems, T. S. Ratiu, ed., Springer-Verlag, New York, 1991, pp. 33–51.

[2] V. I. Arnold, *Mathematical Methods of Classical Mechanics*, Grad. Texts in Math. 60, Springer-Verlag, New York, 1989.

[3] E. Buzano, G. Geymonat, and T. Poston, *Post-buckling behavior of a non-linearly hyperelastic thin rod with cross-section invariant under the dihedral group* D_n, Arch. Ration. Mech. Anal., 89 (1985), pp. 307–388.

[4] P. Chossat and M. Golubitsky, *Symmetry increasing bifurcation of chaotic attractors*, Phys. D, 788 (1988), pp. 423–436.

[5] P. Chossat and R. Lauterbach, *Methods in Equivariant Bifurcation and Dynamical Systems*, Adv. Ser. Nonlinear Dynam. 15, World Scientific, Singapur, 2000.

[6] G. Domokos, *Taylor approximation of operators with discrete rotational symmetry*, Z. Angew. Math. Mech., 72 (1992), pp. 221–225.

[7] Zs. Gaspar and G. Domokos, *Uber das post-kritische Verhalten von Systemen mit C_n-symmetrie*, Z. Angew. Math. Mech., 72 (1992), pp. T110–T111.

[8] H. Goldstein, *Classical Mechanics*, Addison-Wesley, Reading, MA, 1980.

[9] M. Golubitsky, I. Stewart, and D. Schaeffer, *Singularities and Groups in Bifurcation Theory*,

Vol. 2, Appl. Math. Sci. 69, Springer-Verlag, New York, 1988.

[10] F. Grabsi, J. Montaldi, and J.-P. Ortega, *Bifurcation and forced symmetry breaking in Hamiltonian systems*, C. R. Math. Acad. Sci. Paris, 338 (2004), pp. 565–570.

[11] J. Montaldi, *Perturbing a symmetric resonance: The magnetic spherical pendulum*, in STP98 Symmetry and Perturbation Theory II, A. Degasperis and G. Gaeta, eds., World Scientific, River Edge, NJ, 1999, pp. 218–229.

[12] J. Montaldi, M. Roberts, and I. Stewart, *Periodic solutions near equilibria of symmetric Hamiltonian systems*, Philos. Trans. Roy. Soc. London Ser. A, 325 (1988), pp. 237–293.

[13] J. Marsden and T. Ratiu, *Introduction to Mechanics and Symmetry*, 2nd ed., Texts Appl. Math. 17, Springer-Verlag, New York, 1999.

[14] J. M. Wendlandt and J. E. Marsden, *Mechanical integrators derived from a discrete variational principle*, Phys. D, 106 (1997), pp. 223–246.